Oncolytic virotherapy - analysis, design, models

Bhatt, Darshak

DOI:
10.33612/diss.859671389

CHAPTER 8

Modelling the effects of T cell mediated cytotoxicity on oncolytic virotherapy

Darshak K. Bhatt[1], Thijs Janzen[2], Toos Daemen[1], Franz J. Weissing[2]*

1. Department of Medical Microbiology and Infection Prevention, University Medical Center Groningen, University of Groningen, The Netherlands

2. Groningen Institute for Evolutionary Life Sciences, University of Groningen, Groningen, The Netherlands

* Corresponding author

To be submitted

Abstract

Oncolytic virotherapy uses viruses to infect and kill cancer cells. Models for the interplay of tumour growth and infection dynamics reveal that the outcome of virotherapy can be highly stochastic. However, these models do not take account of immune responses that may be triggered by both the presence of cancer cells and the viral infection. To better understand these processes, we added T cell mediated cytotoxicity to a spatially explicit computational model of oncolytic virotherapy. We find that, in general, an efficient immune response has a positive effect on the therapeutic outcome. This, however, is not always the case. In some scenarios where virotherapy alone would be sufficient for complete tumour eradication, the activation of anti-cancer T cell responses restricts the spread of viruses in the tumour, eventually leading to the persistence of a virus-free tumour. Moreover, robust T cell cytotoxicity towards cancer cells, but not infected cells, is critical for successful therapeutic outcomes. By systematically changing the immune parameters of the model, we investigate how the therapeutic outcome depends on the factors determining the efficacy of the immune response. Several of these parameters exhibit a threshold behaviour. For example, the immune response only has a positive therapeutic effect if the maximal level of cytotoxicity exceeds a critical value or if the diffusion rate of inflammatory factors is above a certain threshold value. We conclude that the effects of the immune system on the outcome of oncolytic virotherapy can be surprising and sometimes counterintuitive. The prediction of therapeutic outcomes requires careful consideration of the interplay of spatial tumour growth, viral infection dynamics, and the determinants of the immune response.

Keywords: spatial model, immune response, inflammatory molecules, therapy failure, stochastic outcome

Introduction

Oncolytic virotherapy, a promising approach in cancer treatment, utilizes native or genetically engineered viruses to infect and kill cancer cells.[1] While oncolytic viruses can directly eliminate cancer cells, the activation of immune responses by

infected cells can potentially further enhance the treatment outcomes.[2–4] Therefore, understanding how immune responses are triggered by oncolytic viruses and regulated in the tumour is important for optimising treatment strategy and improving patient outcomes.

The infection of cancer cells by oncolytic viruses triggers a variety of immune responses, including the production of inflammatory molecules, the recruitment and activation of immune cells, the presentation of cancer antigens to T cells, and finally T cell mediated cytotoxic killing of cancer.[4–6] While the significance of the immune response during virotherapy is widely acknowledged, it is not that clear how it affects the therapeutic outcomes.[7–9] For instance, it is poorly understood under which circumstances will immune responses hamper, rather than foster, a positive therapeutic outcome. Moreover, it is not known which specific factors related to the immune response, such as properties of inflammatory molecules, the presence of antigen-specific T cells, and the tumour microenvironment, are critical for the success of virotherapy. Computational models are well-suited for studying this intricate interplay as they enable the evaluation of specific factors while maintaining consistent conditions. This approach facilitates rapid exploration of different scenarios and identification of hidden patterns that determine therapeutic outcomes to oncolytic virotherapy.

Various types of mathematical models have been employed to capture the complex dynamics of immune responses to oncolytic virotherapy. These models have shed light on critical factors influencing treatment outcomes, such as the spatial organisation of the tumour at the time of virotherapy,[10,11] recruitment of immune cells,[11,12] the effect of antiviral immune responses, often characterised by parameters like viral clearance rates or immune-mediated killing of infected cells,[13–15] and similarly the dynamics of anticancer immune responses.[10,14] Additionally, the stochastic nature of the dynamics resulting from virotherapy and immune responses has been highlighted to consider variability in treatment outcomes.[16] Overall, these studies have revealed that the activation of anticancer immune responses correlates with positive therapeutic outcomes, whereas the triggering of antiviral immune responses results in adverse effects on treatment outcomes.[12,15–23] These observations have suggested strategies to improve therapeutic outcomes by regulating antiviral immune responses, designing

"immune-invisible" oncolytic viruses,[24,25] optimising combination therapies,[14,26,27] improving virus delivery,[10] and understanding complex virus-immune interactions.[28,29] Moreover, computational modelling has allowed the simulation of *in silico* clinical trials to evaluate the ability of oncolytic viruses to induce anticancer immunity.[30,31] However, there remain gaps in understanding the factors underlying poor immune responses to these viruses. For example, it is not understood why some patients do not respond favourably to oncolytic virotherapy (despite having anticancer T cells), while others do. Although previous research has explored the role of inflammatory molecules produced by virus-infected cancer cells in modulating anticancer and antiviral immune responses, these investigations have not taken spatial considerations into account. Furthermore, a comprehensive analysis of tumour characteristics, such as the presence of infection-resistant cancer cells, properties of inflammatory molecules released upon infected-cancer cell death, and the spatial regulation of immune responses have not been fully studied.

To fill this gap, we created a cell-based model to explore the dynamics of T cell based immune responses during oncolytic virotherapy. The model builds upon our previous work,[32] designed to study the spatial dynamics of virus-cancer interactions. In the present study, we added immune responses to this model. To understand the impact of pre-existing anticancer T cells and their influence on therapeutic outcomes, we explore the effect of inflammatory molecules on promoting T cell cytotoxicity (e.g. quantity, diffusion rate, half-life, and immunogenicity), and the effect of tumour density-dependent T cell cytotoxicity. For a comprehensive assessment, we also investigate the effect of pre-existing antiviral T cells on overall therapeutic efficacy.

Results

Brief model description

Figure 1 gives an overview of the model. Our previous model,[32] which does not include an immune response, is our point of departure. This model, which is illustrated in Fig. 1B, considers the implication of a virus infection on a tumour that is growing in a 2D or 3D configuration. There are four different cell types:

healthy stromal cells, uninfected but infection-sensitive cancer cells, infection-resistant cancer cells, and infected cancer cells. All cells can divide (if there is space for this) and die, and the birth and death rates may differ between cell types. Infection-sensitive cancer cells can become infected by an oncolytic virus, which is programmed to preferentially target and kill cancer cells while sparing stromal cells. Via mutation, cancer cells can acquire resistance against the virus. In our previous study,[32] we investigated how the outcome of virotherapy depends on key parameters of the model, like the rate of viral spread (b_i) and the death rate of infected cells (d_i). It is an important insight that, due to the stochasticity of all processes in the model, alternative therapeutic outcomes (like total tumour eradication and persistence of an infection-resistant tumour) can occur for the same parameter settings. Accordingly, the model only allows for probabilistic predictions.

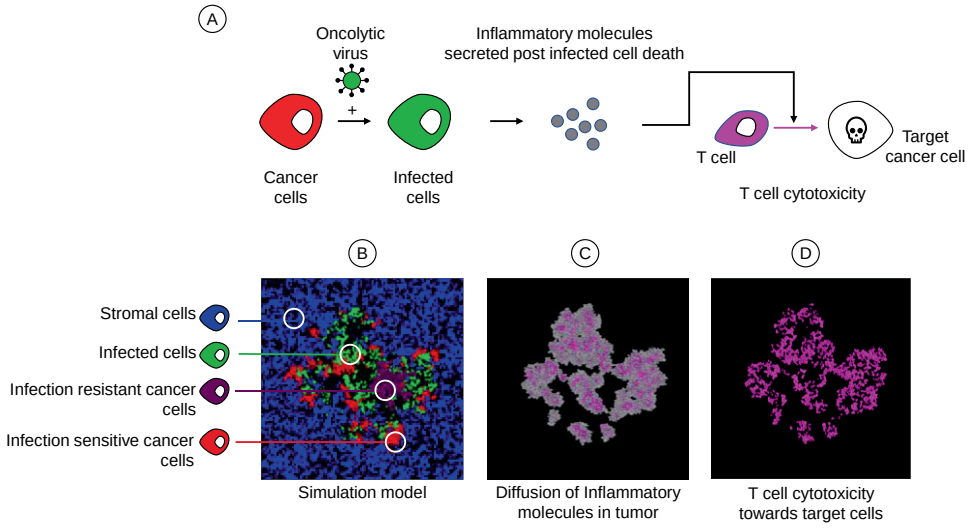

Figure 1: Overview of the model. (A) Crucial events in the model. An infection-sensitive cancer cell (red) can be infected by the virus, turning it into an infected cell (green). When an infected cell dies it releases inflammatory molecules. These molecules induce T cell cytotoxicity, leading to the killing of target cells. (B) Spatial configuration of the model. The model follows the fate of four types of cells: healthy stromal cells (blue), infection-sensitive cancer cells (red), virus-infected cancer cells (green), and resistant cancer cells (purple). Cells divide or die with cell-type specific birth and death rates. Infection-sensitive cancer cells can become infected by virus that is released in the neighbourhood by infected cells. (C) Upon the death of infected cells, inflammatory molecules are released that diffuse in the tumour and eventually evaporate. (D) The local concentration of these molecules serves as a signal to induce T cell cytotoxicity towards target cells in that area.

To assess how the interplay of viral infections and T cell mediated cytotoxicity affects the outcome of oncolytic virotherapy, we here add a cell-specific immune response to the model (Fig. 1A). To this end, we assume that the death of an infected cancer cell results in the release and diffusion of inflammatory molecules in the tumour (Fig. 1C). These inflammatory molecules activate T cells to be cytotoxic towards target cells in the model (e.g. infected cancer cells, but other scenarios are also considered), where the level of cytotoxicity is determined by the local concentration of the molecules (Fig. 1D). Incorporating T cells indirectly in the model, via their cytotoxic effects on various target cells, keeps the model computationally efficient, allowing to investigate a variety of scenarios (with a sufficient number of replicates) on a normal pc.

Average effect of immune response parameters on the outcome of virotherapy

Our model can result in four therapeutic outcomes: (i) total tumour eradication, (ii) partial tumour eradication, (iii) persistence of a virus-susceptible tumour, and (iv) persistence of an infection-resistant tumour. In our previous study,[32] we investigated how the likelihood of each outcome was affected by the properties of the virus and the various cell types and by operational parameters, such as the onset of virotherapy. Figure 2 shows how these likelihoods are modified by the key immune response parameters of our model: the amount of inflammatory molecules released upon the death of an infected cancer cell (λ), the diffusion rate (δ) and the evaporation rate (ε) of inflammatory molecules, the maximal level of cytotoxicity ($\chi_{\max}$), and the EC_{50} value of inflammatory molecules (the concentration of inflammatory molecules at which T cell-mediated cytotoxicity reaches half its maximal value). For each combination of immune response parameters shown, 10,000 simulations were run, for random combinations of two other key parameters of the model: the rate of viral spread (b_i, ranging from 0 to 5) and the death rate of infected cancer cells (d_i, ranging from 0 to 2). This way, Figure 2 indicates the *average* effect of each immune response parameter. Figure 2 shows that for all immune parameters considered the most typical therapeutic outcome is either total tumour eradication (blue) or the persistence of a infection-

sensitive tumour (red). The other two outcomes are less prominent, as they mainly occur for specific regimes of the parameters b_i and d_i (see Bhatt et al. 2022 or Fig. 3A). As one might have expected, the likelihood of the most positive outcome (total tumour eradication) increases with the amount of inflammatory molecules released (Fig. 2A), the diffusion rate of these molecules (Fig. 2B), and the level of cytotoxicity induced by a given concentration of these molecules (Fig. 2D). The likelihood of total tumour eradication decreases with the evaporation rate of inflammatory molecules (Fig. 2C) and the concentration required for an effective immune response (Fig. 2E). Although the direction of these effects is not surprising, the strength of the effect is remarkable. For example, a slight increase in the evaporation rate of inflammatory molecules can shift the likelihood of total tumour eradication from above 50% to almost zero (Fig. 2C).

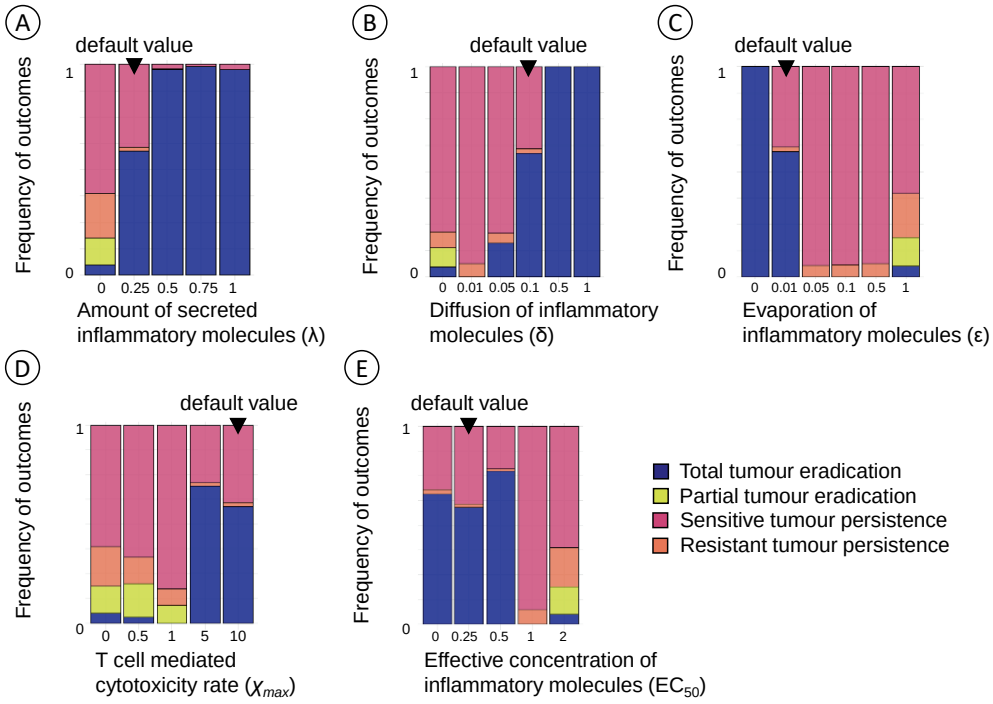

Figure 2: Average effect of the immune response parameters on the therapeutic outcome. Each panel shows how the likelihood of the four outcomes of oncolytic virotherapy is affected by one of the immune response parameters, keeping the other four parameters at their default values. In all cases, the immune response is considered to be non-specific, that is, both infected and uninfected cancer cells are potential targets of T cell cytotoxicity. (A) The likelihood of total tumour eradication increases with the amount λ of inflammatory molecules

released upon the death of an infected cancer cell (default value: $\lambda = 0.25$). (B) The likelihood of total tumour eradication increases with the diffusion rate δ of inflammatory molecules (default value: $\delta = 0.1$). (C) The likelihood of total tumour eradication decreases with the evaporation rate ε of inflammatory molecules (default value: $\varepsilon = 0.01$). (D) The likelihood of total tumour eradication is small for low values of the maximal level of cytotoxicity χ_{max} (the maximal death rate imposed by T cells) but relatively large once χ_{max} increases beyond a threshold value (default value: $\chi_{max} = 10$). (E) The likelihood of total tumour eradication is relatively high for small values of EC50 (the concentration of inflammatory molecules at which T cell-mediated cytotoxicity reaches half its maximal value) but rapidly drops to zero in case of larger EC50 values (default value: $EC_{50} = 0.25$). The likelihood of the four therapeutic outcomes in the absence of an immune response can be deduced from the case $\lambda = 0$ in (A). For each parameter studied per graph, 10,000 simulations were run for various values of the rate of virus spread (bi) and the death rate of infected cancer cells (di), parameters that were drawn at random from a uniform distribution on the parameter range shown in Fig. 3A.

Three scenarios for the effect of immune responses on the outcome of virotherapy

Figure 2 gives an impression of the "typical" effects of T cell mediated cytotoxicity on the outcome of virotherapy. To this end, each data point summarises the effects for a range of values of the parameters b_i (rate of viral spread) and d_i (death rate of virus-infected cancer cells). In Figure 3, we zoom in and consider three specific combinations of b_i and d_i that, in the absence of an immune response, tend to lead to different therapeutic outcomes (Fig. 3A): total tumour eradication by virotherapy alone in Scenario 1, persistence of an infection-resistant tumour in Scenario 2, and persistence of an infection-sensitive tumour in Scenario 3. To these scenarios, we added an immune response. The level of T cell mediated cytotoxicity was systematically changed from low to high by decreasing two immune response parameters of our model (EC_{50} in Fig. 3B; v in Fig. 3C). As a result, the immune response is changed from 'weak' to 'strong' in the graphs of Fig. 3BC. One might have expected that a stronger immune response leads to a more favourable therapeutic outcome.

The graphs for Scenario 1 show that this is not necessarily the case. In this scenario, the likelihood of total tumour eradication (blue curve) is high in the case

of a weak immune response, but it drops with the strength of the immune response. In the case of a strong immune response, the likelihood of tumour eradication is even lower than the likelihood of persistence of an infection-sensitive tumour (red curve). The opposite happens in Scenario 3. Here, the likelihood of tumour persistence is almost one in the case of a weak immune response, while it is exceeded by the likelihood of tumour eradication in the case of a strong immune response. Interestingly, the transition between the two outcomes occurs quite abruptly: for both model parameters (EC_{50} in Fig. 3B; v in Fig. 3C), the likelihood of tumour eradication is close to zero if the parameter is above a certain threshold, while this likelihood 'jumps' to a value above 50% as soon as the parameter drops below the threshold. Regarding tumour eradication, Scenario 2 is very comparable to Scenario 3: the likelihood of eradication is close to zero in the case of a weak immune response (i.e. if the model parameter considered is above a threshold value) and it switches to a value slightly above 0.5 in the case of a strong immune response. Scenario 2 differs from Scenario 3 in what happens in the case of a weak immune response (no tumour eradication). This is best visible in the graph for model parameter EC_{50} (Fig. 3B): if this parameter is close to 2, the most likely therapeutic outcome is the persistence of an infection-resistant tumour; while the most likely outcome is the persistence of an infection-sensitive tumour for a small range of EC_{50} values around 1.0. For model parameter v (Fig. 3C), the overall pattern is similar, but for the range of v-values considered, we did not observe situations where the persistence of an infection-resistant tumour is the most likely outcome. This, however, happens if v is increased beyond the value of 5 (not shown).

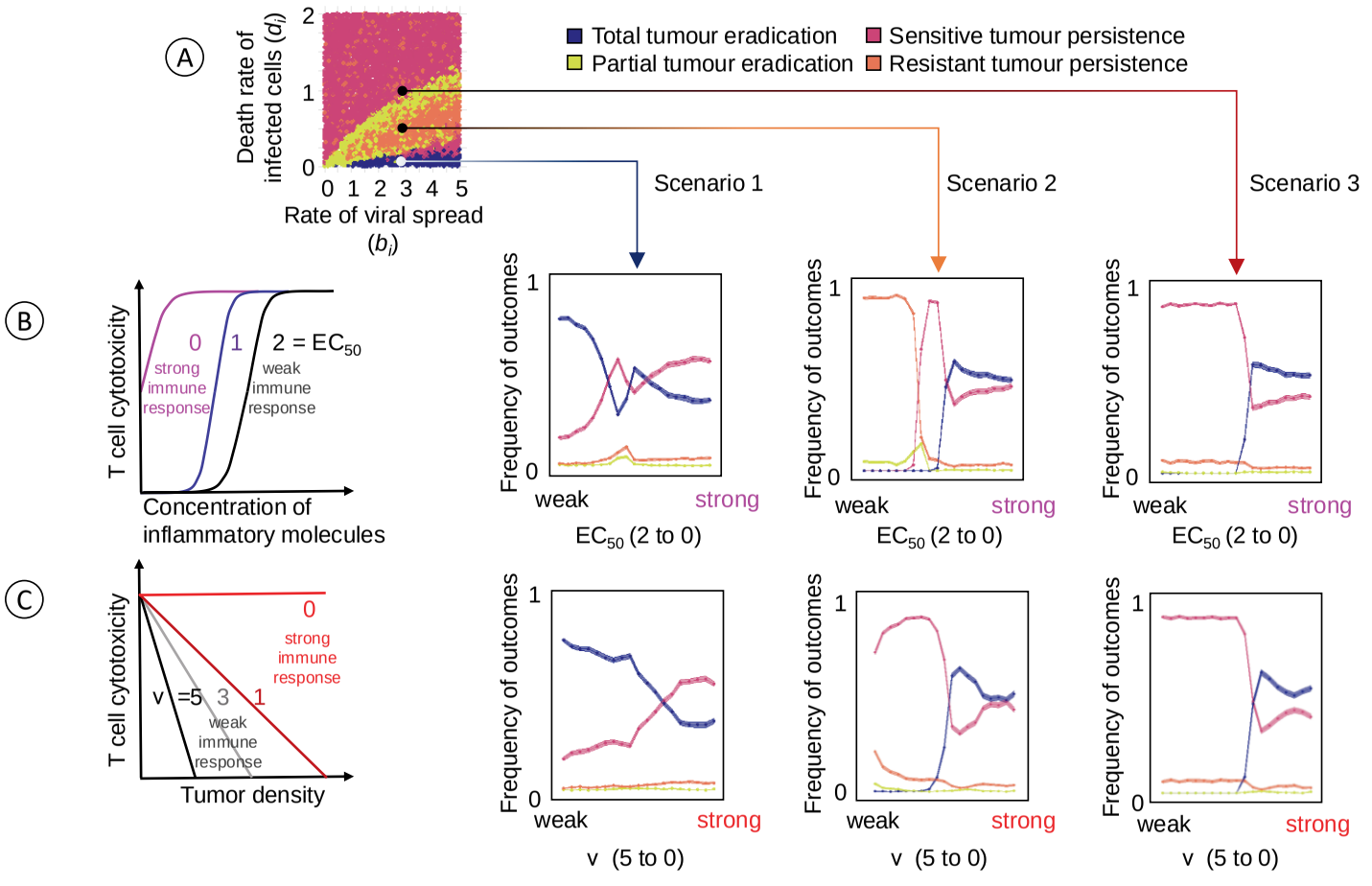
A
Death rate of infected cells (d_i)
Rate of viral spread (b_i)
Total tumour eradication
Partial tumour eradication
Sensitive tumour persistence
Resistant tumour persistence
Scenario 1
Scenario 2
Scenario 3
B
T cell cytotoxicity
0 strong immune response
1
2 = EC50 weak immune response
Concentration of inflammatory molecules
C
T cell cytotoxicity
v =5 3 1
0 strong immune response
weak immune response
Tumor density
Frequency of outcomes
weak
strong
EC50 (2 to 0)
v (5 to 0)

Figure 3: Effect of immune response parameters on the therapeutic outcome in three scenarios. (A) In the absence of immune responses, the likelihood of the four therapeutic outcomes depends on the rate of viral spread (bi) and the death rate of virus-infected cancer cells (di). The effects of an added immune response are explored for three scenarios with low (scenario 1), moderate (scenario 2), and high (scenario 3) death rate di, which in the absence of immune responses tend to result in total tumour eradication, persistence of resistant tumour, and persistence of sensitive tumour, respectively. For each scenario, we assessed the effect of anticancer T cell cytotoxicity on the therapeutic outcome by systematically changing two immune response parameters. (B) Effect of the EC50 value, the concentration of inflammatory molecules at which T cell-mediated cytotoxicity reaches half its maximal value. Large EC50 values indicate a 'weak' immune response in the sense that a high concentration of inflammatory molecules is required to trigger the response. (C) Effect of the model parameter v, which quantifies the negative effect of local tumour density on the effectiveness of the immune response. A larger the value of v indicates a stronger inhibition of the immune response by a high density of tumour cells and, hence, a 'weaker' immune response. Each of the six graphs in (B) and (C) represents 100,000 simulations, where all model parameters were kept at their default values except the ones under investigation. For the parameter under investigation, 1,000 values were chosen at random and 100 replicate simulations were run per chosen value. Coloured lines indicate the mean value, and coloured envelopes indicate the 95% confidence band. Mean and confidence intervals were obtained via nonparametric bootstrapping.

Interestingly, the effect of a parameter change is not necessarily monotonic. This can be seen in Scenario 1 where a decrease of EC_{50} from 2 to 0 (Fig. 3B), the likelihood of tumour eradication (blue curve) first drops rapidly, then increases rapidly, and subsequently decreases gradually.

A detailed view on immune response effects

Figure 4 provides a more detailed view of immune effects on the outcome of virotherapy. Keeping all other immune-related parameters at their default values, the figure considers three values of EC_{50}, the concentration of inflammatory molecules at which T cell-mediated cytotoxicity reaches half its maximal value, and three values of the diffusion rate δ of inflammatory molecules. For each of the nine parameter combinations, many simulations were conducted in order to get an overview of how the therapeutic outcome depends on the rate of viral spread (b_i) and the death rate of virus-infected cancer cells (d_i).

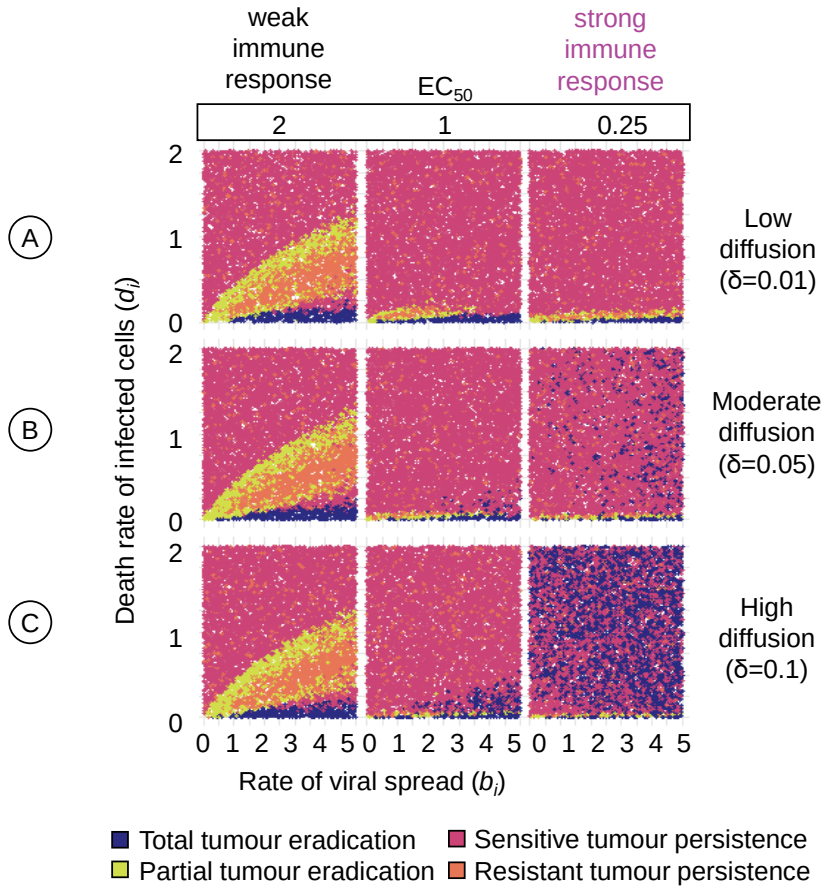

Figure 4: Detailed view of the effect of two immune parameters on the therapeutic outcome. For a range of values of the rate of viral spread (bi) and the death rate of virus-infected cancer cells (di) the panels show how the outcome of oncolytic virotherapy is affected by two immune parameters: the effective concentration of inflammatory molecules (EC50) and the diffusion rate (δ) of these molecules. For three diffusion rates, (A) low ($\delta = 0.01$), (B) moderate ($\delta = 0.05$), and (C) high ($\delta = 0.1$), we assessed the effect of three EC50 values, corresponding to a weak ($EC_{50} = 2$), moderate ($EC_{50} = 1$), and strong ($EC_{50} = 0.25$) immune response. and their effective concentration (EC50) on therapeutic outcomes. The upper left graph resembles Fig. 3A, which depicts the corresponding graph in the absence of an immune response. For each graph in the figure, 10,000 simulations were run for parameter combinations (bi, di) chosen randomly within the specified range. Each simulation is represented by a point, the colour of which indicates the therapeutic outcome. All model parameters were kept at their default values except the ones under investigation.

The three left-most graphs of Fig. 4 correspond to a high value of EC_{50}, indicating a 'weak' immune response (because high concentrations of inflammatory molecules are required to trigger T cell mediated cytotoxicity). Irrespective of the diffusion rate, the same pattern results that is characteristic for the outcome of virotherapy in the absence of an immune response (see Bhatt et al., 2022, and Fig. 3A): the tumour tends to be eradicated (blue dots) for a wedge of parameter combinations that have in common that the death rate d_i of infected cancer cells is very low; an infection-sensitive tumour tends to persist (red dots) when d_i is very high; and the two other outcomes (yellow dots: partial tumour eradication; orange dots: persistence of an infection-resistant tumour) tend to be found for a wedge of parameter combinations for which d_i takes on intermediate values. Interestingly, a somewhat stronger immune response (middle panels, $EC_{50} = 1$) does not lead to a more favourable therapeutic outcome. In comparison to an absent (Fig. 3A) or a weak ($EC_{50} = 2$) immune response, fewer combinations of b_i and d_i lead to total (blue) or partial (yellow) tumour eradication, while most combinations lead to the persistence of an infection-sensitive tumour. On the positive side, therapy rarely leads to the persistence of a tumour that is resistant against virotherapy (orange). Tumour eradication is only boosted if T cell mediated cytotoxicity does not require a high concentration of inflammatory molecules ($EC_{50} = 0.25$) and the diffusion rate of these molecules is high (Fig. 4C) or at least moderate (Fig. 4B). Under these conditions, the tumour can be eradicated even for high values of d_i. However, one needs to keep in mind that the therapeutic outcome is probabilistic and that even under these favourable immune conditions tumour eradication has a similar likelihood as the persistence of an infection-sensitive tumour.

Effects of T cell specificity

Until now, we assumed that T cell mediated cytotoxicity was targeted against infection-sensitive cancer cells. Figure 5 extends the investigation by assessing the therapeutic outcome for six scenarios regarding the specificity of cytotoxicity. The first scenario (no cytotoxicity) corresponds to the absence of an immune response (Bhatt et al., 2022;[32] Fig. 3A) and serves as a standard of comparison.

The fifth scenario (cytotoxicity targeted against infection-sensitive cancer cells) represents our default assumption and was studied above (Fig. 4, $EC_{50} = 0.25$). If cytotoxicity is targeed against infected cells (second scenario), therapy almost always results in the persistence of the tumour. This failure of oncolytic virotherapy is not not surprising if the immune system counteracts viral infection.

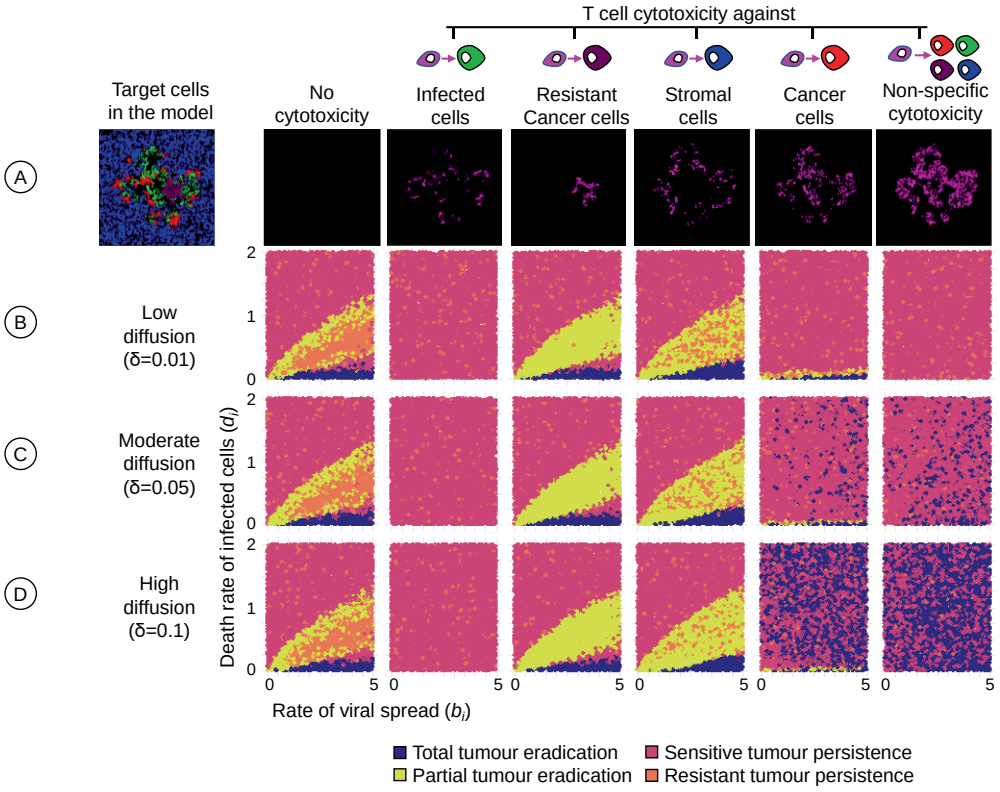

Figure 5: Effect of T cell specificity on the therapeutic outcome. For three diffusion rates of inflammatory molecules, the panels show how the outcome of oncolytic virotherapy is affected if the T cells do not target infection-sensitive cancer cells (the standard scenario) but other cells in the model. (A) The leftmost panel shows a snapshot of the potential target cells: healthy stromal cells (blue), uninfected but infection-sensitive cancer cells (red), infection-resistant cancer cells (purple), and infected cells (green). The other panels show snapshots of the distribution of inflammatory molecules for the six scenarios considered: no cytotoxicity (absence of an immune response), and T cell cytotoxicity targeted towards either (from left to right) infected cells, infection-resistant cancer cells, stromal cells, infection-sensitive cancer cells, or all cell types present. The six scenarios were studied for three diffusion rates: (B) low ($\delta = 0.01$), (C) moderate ($\delta = 0.05$), and (D) high ($\delta = 0.1$). For each graph in the figure, 10,000 simulations were run for parameter combinations (bi, di) chosen randomly within the specified range. Each simulation is represented by a point,

the colour of which indicates the therapeutic outcome. All model parameters were kept at their default values except the ones under investigation.

In contrast to the second scenario, the immune response can have a postive effect on the therapeutic outcome (a higher likelihood of total or partial tumour eradication) if it is targeted against infection-resistant cancer cells (third scenario) or against healthy stromal cells (fourth scenario). Targeting stromal cells can be beneficial because these cells can prevent the effective spread of the virus by creating spatial barriers as observed by us previously.[32] The same applies when resistant cancer cells are targeted; here, the targeting of resistant cells can prevent the most unfavourable outcome of virotherapy: the persistence of an infection-resistant tumour. In both scenarios, the positive effect of the immune system is restricted to combinations of b_i and d_i where the death rate d_i of virus-infected cancer cells is relatively low. For those combinations of b_i and d_i where, in the absence of an immune response, virotherapy resulted in the persistence of an infection-sensitive tumour (red areas in the graphs of the left column of Fig. 5), the same outcome also resulted in the third and fourth scenario. Our model predicts that an unspecifc immune response (sixth scenario) has a similar of even a more favourable effect on therapeutic outcome as a response targeted against infection-resistant cancer cells (fifth scenario). Interestingly, in both scenarios the therapeutic outcome is typically worse than the outcome in the absence of an immune response (first scenario) if the diffusion rate of inflammatory molecules is low. This suggests that an efficient immune response throughout the tumour, facilitated by high diffusion rates, is crucial for achieving successful treatment outcomes. This was also the case when we simulated scenarios where T cell cytotoxicity was directed towards multiple cell types simultaneously (Supplementary Figure S2) or in the setting of a 3D model (Supplementary Figure S3).

Discussion

In this study, we investigated the dynamics of immune responses during oncolytic virotherapy using a spatially explicit computational modelling approach. We explored the effects of inflammatory molecules, target-specific immune

responses, and tumour density-dependent immune inhibition in regulating therapeutic efficacy of oncolytic viruses. Our results show that for a wide range of scenarios, immune responses can aid oncolytic viruses in total tumour eradication, but only when two conditions are met: the immune response has to be cancer-specific and inflammatory molecules have to be effective and spread fast. Alternatively, strong antiviral immune responses and weak anticancer immune responses due to tumour-density effects limit the therapeutic efficacy of oncolytic viruses. Overall, our findings provide insights into the interplay between T cell mediated immune response to oncolytic viruses.

Various experimental and computational studies have noted the disadvantages of eliciting antiviral immune responses as they act against the tumour-killing potential of virotherapy.[12,15–23] In our model, we replicate these findings and explain why this happens. When T cell cytotoxicity is directed towards only infected cells, we find that even a weak cytotoxic activity leads to a rapid clearance of infected cells thus resulting in a limited spread of oncolytic viruses (Figure 5). The elimination of infected cells reduces the persistence of virus in the tumour and undermines favourable therapeutic outcomes. Interestingly, under some conditions, immune responses can be beneficial for the therapeutic outcome even if they are directed against infected cells. For instance, when T cell cytotoxicity is directed towards cancer cells in addition to infected cells it leads to an increase in the likelihood of total tumour eradication (Supplementary Figure 2). However, this is only possible when inflammatory molecules diffuse at a faster rate in the tumour.

The activation of anticancer immune responses has been generally considered to be a positive factor for total tumour eradication.[2,33] However, we show that T cell cytotoxicity towards cancer cells may also lead to poor therapeutic outcomes by limiting virus spread in the tumour. We find that when T cell cytotoxicity is directed towards infection-susceptible cancer cells surrounding infected cells, it eliminates potential target cells that could enable efficient virus spread in the tumour. The spatial barriers resulting from anticancer T cell cytotoxicity lead to poor persistence of the virus in the tumour and thus undermine favourable therapeutic outcomes. This effect is observed to be significant for oncolytic viruses spreading at a rapid rate and infected cells die at a slow rate (Figure 3, scenario 1). Low

diffusion rates of inflammatory molecules lead to similar effects, keeping the T cell response restricted to the neighbourhood of infected cells, thereby again creating spatial barriers to local viral spread. When virotherapy alone is sufficient to eradicate cancer, T cell killing of cancer cells may limit the spread of virus in the tumour and eventually lead to the persistence of a virus-free tumour. Thus, our results identify potential confounding factors that could help explain therapeutic outcomes where a tumour can persist despite activation of anticancer T cells by oncolytic virotherapy.

The inclusion of spatial considerations in our model extends the existing work on modelling immune responses or T cell responses to oncolytic viruses.[12,14–23] Spatial modelling allows for the ability to capture the complex dynamics of oncolytic virotherapy within the tumour microenvironment. In particular, the diffusion of inflammatory molecules plays a key role in controlling the impact of T cell cytotoxicity and, thus, affects the overall therapeutic results. High diffusion rates facilitate extensive spread of inflammatory molecules, ensuring widespread T cell activation and enhancing therapeutic efficacy. However, it is crucial to strike a balance, as too much diffusion, in combination with a high EC_{50}, can lead to a rapid spread of inflammatory molecules with suboptimal effects (Figure 4). Conversely, low diffusion restricts the reach of these molecules, leading to localized T cell activation and potential impairment of the immune response. Likewise, it is crucial to consider the diffusion rate along with the evaporation rate of inflammatory molecules, as they determine, respectively, the spatial and temporal activation of immune responses in the tumour. This observation aligns with the finding of Centofanti and colleagues that immune-mediated tumour cell clearance is spatially regulated due to the diffusion-consumption dynamics of inflammatory molecules within the tumour tissue.[34]

Tumour density mediated regulation of immune responses has been noted as an important factor that restricts cancer eradication.[35–38] However, we observe that this is not always the case. When tumour density effect strongly inhibits T cell cytotoxicity towards cancer cells, we find that there is an increase in likelihood of total tumour eradication when the oncolytic virus spreads at a faster rate and infected cells die at a slow rate (Figure 3, scenario 1). In this case, the anticancer T cell cytotoxicity does not limit the viral spread by targeting neighbouring

infection-susceptible cells and allows efficient elimination of tumour. Tumour density mediated suppression of T cell cytotoxicity leads to a decrease in the likelihood of total tumour eradication only when the virus alone is unable to eliminate the tumour and requires strong activation of immune responses (Figure 3, scenario 2 and 3). Experimental observations so far have revealed that T cell activity reduces with increasing tumour density due to a hypoxic microenvironment, high expression of immunosuppressive molecules and low nutrient availability.[36,39–41] Therefore, for factors such as hypoxia and low nutrient availability, which also influence the properties of the virus, the activation of immune responses may prove to be critical to achieve favourable therapeutic outcomes.[38]

The properties of the inflammatory molecules released by infected cells have a strong impact on regulating the immune responses and thereby the therapeutic outcomes. For instance, our results demonstrate that the value of the effective concentration of inflammatory molecules required to induce T cell cytotoxicity, EC_{50}, determines if T cell responses favour oncolytic virotherapy or not. We find that highly effective inflammatory molecules, with a low EC_{50} value, are necessary when virotherapy alone does not yield total tumour eradication. This observation has been made numerously, where high affinity immunostimulatory molecules like cytokines or checkpoint inhibitors can improve the cytotoxicity of anticancer T cells within the tumour, thereby improving tumour eradication.[42,43] Considering the EC50 of inflammatory molecules with the diffusion and evaporation rates, our findings suggest a spectrum of optimal attributes that inflammatory molecules should exhibit to effectively facilitate complete tumour eradication following virotherapy.

Knowledge about the optimal attributes of inflammatory molecules can be especially important when engineering oncolytic viruses to encode immune-stimulatory genes like cytokines, chemokines, or T-cell engager proteins. T-cell engager proteins, exemplified by Bispecific T cell engagers (BiTEs), possess dual binding domains: one attaches to a T cell receptor, while the other targets a cancer cell antigen. This interaction brings T cells into direct contact with cancer cells, activating T cells to effectively eliminate the cancer cells.[44,45] Considering T-cell engager proteins as the inflammatory molecules released by infected cells,[46] our

model provides two recommendations for improving the design of these molecules. Firstly, effectiveness of BiTEs could be improved by restricting the specificity of the binding antigen, in order to avoid targeting infected cells, which we have found would greatly impair the effectivity of the treatment. Secondly, the effectivity of BiTEs could be improved by increasing diffusion across cells and reducing the breakdown over time of BiTEs. The breakdown of BiTEs can be improved by directed evolution and screening of BiTEs resistant to enzymatic or physiological degradation, whereas the diffusion of BiTEs can be improved by engineering smaller and low molecular weight BiTEs or by reducing the extracellular matrix density through enzymatic activity mediated by infected cells.[45,47–50]

Our study was primarily focused to investigate the role of inflammatory molecules as regulators of immune response in the tumour and their influence on therapeutic outcomes. While this approach offers valuable insights, it represents just one facet of the immune response to cancer and may not comprehensively capture the complexity of the immune-tumour interactions. Future research should aim to explore a broader spectrum of factors and interactions within the immune system to obtain a more comprehensive understanding of cancer therapy outcomes. A more direct integration of individual T cells and other immune cells into our model may elucidate unexplained preclinical and clinical observations. Potential avenues of expansion of the model include the impact of T cell migration and tumour-infiltration on tumour regression, the role of tumour-associated macrophages in immune modulation, and the cross-talk between antigen presenting cells and T cells for antigen-specific killing. Understanding these dynamics can lead to identifying therapeutic targets and strategies focused on enhancing T cell recruitment or modulating macrophage activation for improved treatment outcomes. Such a comprehensive model holds the promise to advance oncolytic virotherapy's efficacy and provide valuable insights into tumour-immune interactions.

Model description

To assess the effect of immune responses on the outcome of oncolytic virotherapy, we added T cell mediated cytotoxicity to the model of Bhatt et al. (2022).[32] A flow chart of the model can be found in Supplementary Figure S1.

Brief overview of the model of Bhatt et al. (2022)

The model of Bhatt et al. (2022)[32] considers the growth of cancer and stromal cells and the dynamics of a viral infection on a spatial grid, using an event-based time structure. The spatial grid consists of 'grid cells' that can either be empty or harbour cancer or stromal cells. Simulations can be run for three spatial configurations: a regular 3D grid, a regular 2D grid, and a more natural 2D Voronoi grid. Unless mentioned otherwise (see Supplementary Figure S3 for 3D simulations), all simulations reported here were run on a 2D Voronoi grid. The model assumes that stromal and cancer cells can divide (produce a daughter that is placed into an empty neighbouring grid cell, provided that such a grid cell exists) and that cancer cells can become infected by an oncolytic virus, which is programmed to preferentially target and kill cancer cells while sparing stromal cells. By means of rare mutations, cancer cells can acquire resistance against the oncolytic virus. Hence, the model considers four different cell types: healthy stromal cells, uninfected but infection-sensitive cancer cells, infection-resistant cancer cells, and infected cancer cells. All these cells can die; and the death rate may depend on the type of cell. In the simulations reported here, all cell-type specific parameters are at their default values (Table 1 in Bhatt et al., 2022)[32], with the exception of the rate of viral spread (b_i) and the death rate of infected cells (d_i), which are varied as indicated in the figure legends.

In this model, each simulation results in one of the following four outcomes: complete eradication of the tumour, partial eradication of the tumour, persistence of an infection-sensitive tumour, and persistence of an infection-resistant tumour. Due to the stochasticity of all processes in the model, alternative therapeutic outcomes can occur for the same parameter settings. It is therefore important to run multiple replicate simulations for each parameter combination in order to get a good overview (like Fig. 3A) on how the likelihood of the various outcomes depend on the model parameters.

Adding T cell mediated cytotoxicity to the model

We adopt an indirect approach to incorporate T cell mediated cytotoxicity in the model. Instead of explicitly simulating the dynamics of individual T cells, we assume that the death of an infected cancer cell results in the release and diffusion of inflammatory molecules in the tumour. These inflammatory molecules serve as a proxy for T cell activity, such that higher local concentrations of these molecules increase the degree of T cell-mediated cytotoxicity, resulting in higher cell death rates. By default, we assume that cytotoxicity is targeted against cancer cells, but other options are also considered (e.g. in Fig. 5).

To be more precise, we assume that inflammatory molecules are absent at the start of a simulation. Whenever an infected cancer cell dies, the amount (or, equivalently, the concentration) of inflammatory molecules in the corresponding grid cell is increased by λ. The inflammatory molecules do not stay indefinitely in the grid cell, but rather disperse to neighbouring grid cells following diffusion dynamics or slowly disappear due to evaporation. Diffusion is modelled as follows: at fixed time intervals *dt* (default value $dt = 0.01$ days), a fraction δ of the local inflammatory molecules 'disperse away' to the neighbouring cells, while at the same time new molecules are gained via dispersal from the neighbouring cells. If $\eta(t)$ is the concentration of these molecules in a focal grid cell at time *t* and $\eta_j(t)$ is the concentration in the *n* neighbouring cells $j = 1,\ldots,n$ at this time, then the concentration in the focal cell changes as follows:

$$\eta(t+dt) = (1-\delta)\cdot\eta(t) + \delta\cdot\sum_j \eta_j(t)/n_j \,,$$

where n_j is the number of grid cells neighbouring grid cell *j*. After diffusion has taken place in the whole grid, the concentration of inflammatory molecules in each grid cell is reduced by a factor 1-ε, corresponding to the evaporation of a fraction ε of these molecules. Concentrations below 10^{-5} were set to zero. We implemented diffusion and evaporation at fixed time intervals *dt* in order to reduce the computational strain on the model. The parameters δ and ε are fractions of molecules lost per time interval *dt* and should be interpreted correspondingly. If

the time interval is changed by a factor κ, δ and ε should be changed accordingly: if, for example, *dt* is increased from its default value 0.01 to 0.05, the default values of δ and ε should also be increased by the factor 5: from $\delta = 0.1$ to $\delta = 0.5$ and from $\varepsilon = 0.01$ to $\varepsilon = 0.05$.

Cytotoxicity is included in the model by increasing the mortality of the target cells by an amount $\chi(\eta)$, which is dependent on the local concentration η of the inflammatory molecules. As a default, we assume that $\chi(\eta)$ is given by the logistic function:

$$\chi(\eta) = \chi_{\max} / (1 + \exp(\mathrm{EC}_{50} - \eta)) .$$

In other words T cell induced mortality increases with η in an S-shaped manner, asymptotically approaching the maximal value $\chi_{\max}$. These assumptions are motivated by the fact that T cells are activated in a dose-dependent manner upon stimulation with inflammatory signals such as cognate antigens, T cell engager molecules or cytokines.[51–54] The parameter EC_{50} corresponds to that concentration η at which the T cell mediated cytotoxicity reaches 50% of its maximal value: $\chi(\mathrm{EC}_{50}) = \frac{1}{2}\chi_{\max}$. Therefore, EC_{50} may be viewed as the 'effective' concentration of inflammatory molecules, that is, the concentration required to launch an effective immune response. If EC_{50} is small, the immune system responds to the inflammatory molecules in a highly sensitive manner; if EC_{50} is large, an effective immune response required a large accumulation of inflammatory molecules.

The model also includes the option that cancer cells that are located at the periphery of the tumour experience a higher T cell-mediated mortality than cancer cells located more centrally in the tumour. The reason is that more centrally located target cells are more difficult to reach by the immune system. To model this, we expanded the expression of $\chi(\eta)$ by a density dependent term:

$$\chi(\eta, \Phi) = (1 - \nu\,\Phi) \cdot \chi_{\max} / (1 + \exp(\mathrm{EC}_{50} - \eta)) .$$

Here, Φ denotes the relative density of cancer cells in the neighbourhood (the fraction of neighbouring grid cells occupied by cancer cells) while v indicates the strength of the density effect. As default, we chose $\nu = 0$, corresponding to the absence of a density effect.

Table 1: Parameters related to T cell mediated cytotoxicity, their default values, and the range of values investigated in the simulations. All other model parameters and their default values can be found in Table 1 in Bhatt et al. (2022)[32]

Parameter	*Interpretation*	*Default value*	*Evaluated range*
λ	Amount of inflammatory molecules released by an infected cell upon death	0.25	0 to 1
dt	Time interval between diffusion and evaporation events [unit: days]	0.01	0.01
δ	Diffusion rate: fraction of molecules that disperse to neighbouring grid cells per time interval *dt*	0.1	0 to 0.1
ε	Evaporation rate: fraction of molecules that disappear due to evaporation or breakdown per time interval *dt*	0.01	0 to 0.1
χ_{max}	Maximum cytotoxicity (T cell mediated death rate of cancer cells or other target cells of the immune system)	10	0 to 10
EC_{50}	Concentration of inflammatory molecules at which cytotoxicity reaches 50% of χ_{max}	0.25	0 to 2
ν	Strength of the inhibitory effect of tumour density on cytotoxicity	0	0 to 5

Data Availability Statement

To improve usability, we provide two different versions of the model for all common operating systems: 1) a terminal-only version, which reads parameters from a configuration file and which can be used to perform demanding simulations

on a high-performance computation cluster and 2) a graphical version, where the user is provided with an intuitive graphical user interface and can visually observe the spatial interplay between cell types. The code used for this work and an executable version of the Oncolytic Virus Resistance and Immune simulator (OVRI) will be made available on www.github.com/rugtres.

Funding

The work of FJW is supported by the European Research Council (ERC Advanced Grant No. 789240). D.K.B. received a PhD scholarship from CAPES (Finance Code 001) and ATTP-GSMS (Abel Tasman Talent Program) Groningen.

Competing Interests

The authors declare that there are no competing interests.

Author contributions

Conceptualization: DKB, TJ, TD, FJW; Implementation: TJ, DKB; Model analysis: DKB; Writing: DKB, TJ, TD, FJW

References

1. Kelly, E. & Russell, S. J. History of Oncolytic Viruses: Genesis to Genetic Engineering. *Molecular Therapy* **15**, 651–659 (2007).
2. Martin, N. T. & Bell, J. C. Oncolytic Virus Combination Therapy: Killing One Bird with Two Stones. *Molecular Therapy* **26**, 1414–1422 (2018).
3. Russell, S. J., Peng, K.-W. & Bell, J. C. Oncolytic virotherapy. *Nat Biotechnol* **30**, 658–670 (2012).
4. Kaufman, H. L., Kohlhapp, F. J. & Zloza, A. Oncolytic viruses: a new class of immunotherapy drugs. *Nature Reviews Drug Discovery* **14**, 642–662 (2015).
5. Kaufman, H. L. *et al.* Local and Distant Immunity Induced by Intralesional Vaccination with an Oncolytic Herpes Virus Encoding GM-CSF in Patients with Stage IIIc and IV Melanoma. *Ann Surg Oncol* **17**, 718–730 (2010).
6. Twumasi-Boateng, K., Pettigrew, J. L., Kwok, Y. Y. E., Bell, J. C. & Nelson, B. H. Oncolytic viruses as engineering platforms for combination immunotherapy. *Nat Rev Cancer* **18**, 419–432 (2018).
7. Ma, R., Li, Z., Chiocca, E. A., Caligiuri, M. A. & Yu, J. The emerging field of oncolytic virus-based cancer immunotherapy. *Trends Cancer* **9**, 122–139 (2023).
8. Shalhout, S. Z., Miller, D. M., Emerick, K. S. & Kaufman, H. L. Therapy with oncolytic viruses: progress and challenges. *Nat Rev Clin Oncol* **20**, 160–177 (2023).
9. Moaven, O., W Mangieri, C., A Stauffer, J., Anastasiadis, P. Z. & Borad, M. J. Evolving Role of Oncolytic Virotherapy: Challenges and Prospects in Clinical Practice. *JCO Precis Oncol* **5**, PO.20.00395 (2021).
10. Storey, K. M. & Jackson, T. L. An Agent-Based Model of Combination Oncolytic Viral Therapy and Anti-PD-1 Immunotherapy Reveals the Importance of Spatial Location When Treating Glioblastoma. *Cancers* **13**, 5314 (2021).
11. Jenner, A. L. *et al.* Agent-based computational modeling of glioblastoma predicts that stromal density is central to oncolytic virus efficacy. *iScience* **25**, 104395 (2022).
12. Storey, K. M., Lawler, S. E. & Jackson, T. L. Modeling Oncolytic Viral Therapy, Immune Checkpoint Inhibition, and the Complex Dynamics of Innate and Adaptive Immunity in Glioblastoma Treatment. *Front. Physiol.* **11**, 151 (2020).
13. Mahasa, K. J., Eladdadi, A., de Pillis, L. & Ouifki, R. Oncolytic potency and reduced virus tumor-specificity in oncolytic virotherapy. A mathematical modelling approach. *PLoS One* **12**, e0184347 (2017).
14. Huang, H. *et al.* Oncolytic adenovirus programmed by synthetic gene circuit for cancer immunotherapy. *Nat Commun* **10**, 4801 (2019).
15. Kim, Y. *et al.* Complex role of NK cells in regulation of oncolytic virus–bortezomib therapy. *Proc. Natl. Acad. Sci. U.S.A.* **115**, 4927–4932 (2018).
16. Camara, B. I., Mokrani, H., Diouf, A., Sané, I. & Diallo, A. S. Stochastic model analysis of cancer oncolytic virus therapy: estimation of the extinction mean times and their probabilities. *Nonlinear Dyn* **107**, 2819–2846 (2022).
17. Vithanage, G. V. R. K., Wei, H.-C. & Jang, S. R.-J. Bistability in a model of tumor-immune system interactions with an oncolytic viral therapy. *Math Biosci Eng* **19**, 1559–1587 (2022).
18. Yu, J.-L., Jang, S. R.-J. & Liu, K.-Y. Exploring the Interactions of Oncolytic Viral Therapy and Immunotherapy of Anti-CTLA-4 for Malignant Melanoma Mice Model. *Cells* **12**, 507 (2023).
19. Application of control theory in a delayed-infection and immune-evading oncolytic virotherapy. *Mathematical Biosciences and Engineering* **17**, 2361–2383 (2020).
20. Wang, Z. *et al.* A mathematical model of oncolytic virotherapy with time delay. *Mathematical Biosciences and Engineering* **16**, 1836–1860 (2019).
21. Timalsina, A., Tian, J. P. & Wang, J. Mathematical and Computational Modeling for Tumor Virotherapy with Mediated Immunity. *Bull Math Biol* **79**, 1736–1758 (2017).
22. Al-Tuwairqi, S. M., Al-Johani, N. O. & Simbawa, E. A. Modeling dynamics of cancer virotherapy with immune response. *Adv Differ Equ* **2020**, 438 (2020).

23. Elaiw, A. M. & Al Agha, A. D. A reaction–diffusion model for oncolytic M1 virotherapy with distributed delays. *Eur. Phys. J. Plus* **135**, 117 (2020).
24. Almuallem, N., Trucu, D., Eftimie, R., & Department of Mathematics, University of Dundee, Dundee, DD1 4HN, UK. Oncolytic viral therapies and the delicate balance between virus-macrophage-tumour interactions: a mathematical approach. *Mathematical Biosciences and Engineering* **18**, 764–799 (2021).
25. Mahasa, K. J. *et al.* Mesenchymal stem cells used as carrier cells of oncolytic adenovirus results in enhanced oncolytic virotherapy. *Sci Rep* **10**, 425 (2020).
26. Handoko, H., Wahyudi, S. T., Setyawan, A. A. & Kartono, A. A dynamical model of combination therapy applied to glioma. *J Biol Phys* **48**, 439–459 (2022).
27. Friedman, A. & Lai, X. Combination therapy for cancer with oncolytic virus and checkpoint inhibitor: A mathematical model. *PLoS ONE* **13**, e0192449 (2018).
28. Eftimie, R. & Eftimie, G. Investigating Macrophages Plasticity Following Tumour–Immune Interactions During Oncolytic Therapies. *Acta Biotheor* **67**, 321–359 (2019).
29. Cassidy, T. & Humphries, A. R. A mathematical model of viral oncology as an immuno-oncology instigator. *Mathematical Medicine and Biology: A Journal of the IMA* dqz008 (2019) doi:10.1093/imammb/dqz008.
30. Cassidy, T. & Craig, M. Determinants of combination GM-CSF immunotherapy and oncolytic virotherapy success identified through in silico treatment personalization. *PLoS Comput Biol* **15**, e1007495 (2019).
31. Jenner, A. L., Cassidy, T., Belaid, K., Bourgeois-Daigneault, M.-C. & Craig, M. In silico trials predict that combination strategies for enhancing vesicular stomatitis oncolytic virus are determined by tumor aggressivity. *J Immunother Cancer* **9**, e001387 (2021).
32. Bhatt, D. K., Janzen, T., Daemen, T. & Weissing, F. J. Modelling the spatial dynamics of oncolytic virotherapy in the presence of virus-resistant tumour cells. *PLoS Comput Biol* **18**, e1010076 (2022).
33. Sivanandam, V., LaRocca, C. J., Chen, N. G., Fong, Y. & Warner, S. G. Oncolytic Viruses and Immune Checkpoint Inhibition: The Best of Both Worlds. *Molecular Therapy - Oncolytics* **13**, 93–106 (2019).
34. Centofanti, E. *et al.* The spread of interferon-γ in melanomas is highly spatially confined, driving nongenetic variability in tumor cells. *Proc Natl Acad Sci U S A* **120**, e2304190120 (2023).
35. Davern, M. *et al.* Nutrient deprivation and hypoxia alter T cell immune checkpoint expression: potential impact for immunotherapy. *J Cancer Res Clin Oncol* (2022) doi:10.1007/s00432-022-04440-0.
36. Baldominos, P. *et al.* Quiescent cancer cells resist T cell attack by forming an immunosuppressive niche. *Cell* **185**, 1694-1708.e19 (2022).
37. Hanahan, D. Hallmarks of Cancer: New Dimensions. *Cancer Discovery* **12**, 31–46 (2022).
38. DePeaux, K. & Delgoffe, G. M. Metabolic barriers to cancer immunotherapy. *Nat Rev Immunol* **21**, 785–797 (2021).
39. Hammerl, D. *et al.* Spatial immunophenotypes predict response to anti-PD1 treatment and capture distinct paths of T cell evasion in triple negative breast cancer. *Nat Commun* **12**, 5668 (2021).
40. Wang, X. Q. *et al.* Spatial predictors of immunotherapy response in triple-negative breast cancer. *Nature* **621**, 868–876 (2023).
41. You, R. *et al.* Active surveillance characterizes human intratumoral T cell exhaustion. *J Clin Invest* **131**, e144353 (2021).
42. Maute, R. L. *et al.* Engineering high-affinity PD-1 variants for optimized immunotherapy and immuno-PET imaging. *Proc. Natl. Acad. Sci. U.S.A.* **112**, (2015).
43. Deckers, J. *et al.* Engineering cytokine therapeutics. *Nat Rev Bioeng* **1**, 286–303 (2023).
44. Arvedson, T. *et al.* Targeting Solid Tumors with Bispecific T Cell Engager Immune Therapy. *Annu. Rev. Cancer Biol.* **6**, 17–34 (2022).
45. Goebeler, M.-E. & Bargou, R. C. T cell-engaging therapies — BiTEs and beyond. *Nat Rev Clin Oncol* **17**, 418–434 (2020).

46. Freedman, J. D. *et al.* An Oncolytic Virus Expressing a T-cell Engager Simultaneously Targets Cancer and Immunosuppressive Stromal Cells. *Cancer Research* **78**, 6852–6865 (2018).
47. Li, H., Er Saw, P. & Song, E. Challenges and strategies for next-generation bispecific antibody-based antitumor therapeutics. *Cell Mol Immunol* **17**, 451–461 (2020).
48. English, J. G. *et al.* VEGAS as a Platform for Facile Directed Evolution in Mammalian Cells. *Cell* **178**, 748-761.e17 (2019).
49. Liang, M. *et al.* Targeting matrix metalloproteinase MMP3 greatly enhances oncolytic virus mediated tumor therapy. *Transl Oncol* **14**, 101221 (2021).
50. Kiyokawa, J. *et al.* Modification of Extracellular Matrix Enhances Oncolytic Adenovirus Immunotherapy in Glioblastoma. *Clin Cancer Res* **27**, 889–902 (2021).
51. Weigelin, B. *et al.* Cytotoxic T cells are able to efficiently eliminate cancer cells by additive cytotoxicity. *Nat Commun* **12**, 5217 (2021).
52. Huang, G. L. *et al.* A multivariate, quantitative assay that disentangles key kinetic parameters of primary human T cell function in vitro. *PLoS ONE* **15**, e0241421 (2020).
53. Smith, E. J. *et al.* A novel, native-format bispecific antibody triggering T-cell killing of B-cells is robustly active in mouse tumor models and cynomolgus monkeys. *Sci Rep* **5**, 17943 (2015).
54. Ghaffari, S. *et al.* Optimizing interleukin-2 concentration, seeding density and bead-to-cell ratio of T-cell expansion for adoptive immunotherapy. *BMC Immunol* **22**, 43 (2021).

Supplementary figures

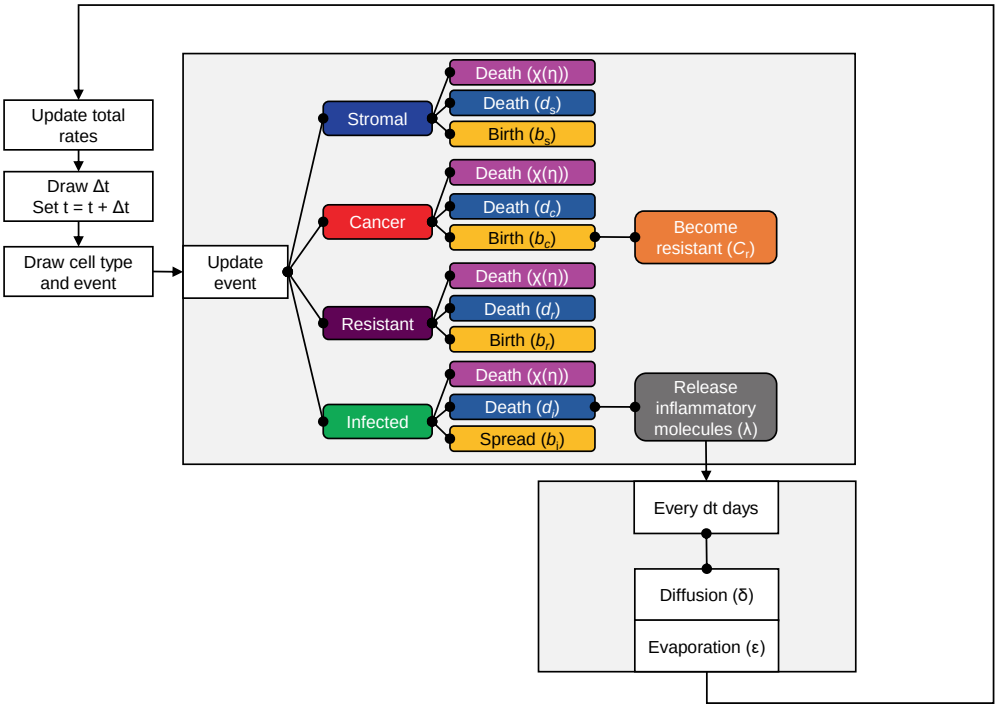

Supplementary Figure 1: Flow diagram of the model. The event-based computational model employs a Gillespie algorithm to simulate the dynamics of virus-cell interactions along with the effect of an immune response. The model consists of stromal cells, virus-infected cells, infection-sensitive cancer cells, and infection-resistant cancer cells. Stromal and cancer cells can proliferate at rates (bs=0.5) and (bc=1.0) respectively, while virus-infected cells can spread the virus to adjacent infection-sensitive cells at specific rates (bi). Infection sensitive cancer cells divide and give rise to resistant cells with a probability (Cr=10-5). Resistant cells proliferate at (br=0.9), which is slightly slower than infection-sensitive cancer cells due to an assumed cost of resistance. Similarly, stromal cells die at death rate (ds=0.2), cancer cells at (dc=0.1), resistant cancer cells at (dr=0.2) and infected cells at (di). For infected cells a range of parameter values are explored, where (di) ranges from 0 to 2 and (bi) ranges from 0 to 5. Upon death, infected cells release (λ) amount of inflammatory molecules, which can then diffuse at a rate (δ) and evaporate at rate (ε) from the model. When the immune response is active, the cells can be either sensitive or resistant to T cell mediated cytotoxicity, where only sensitive cells die at an elevated death rate χ(η). All the rates in the model are expressed in events per day, except diffusion and evaporation rates of inflammatory molecules which update every (dt=10-2) day.

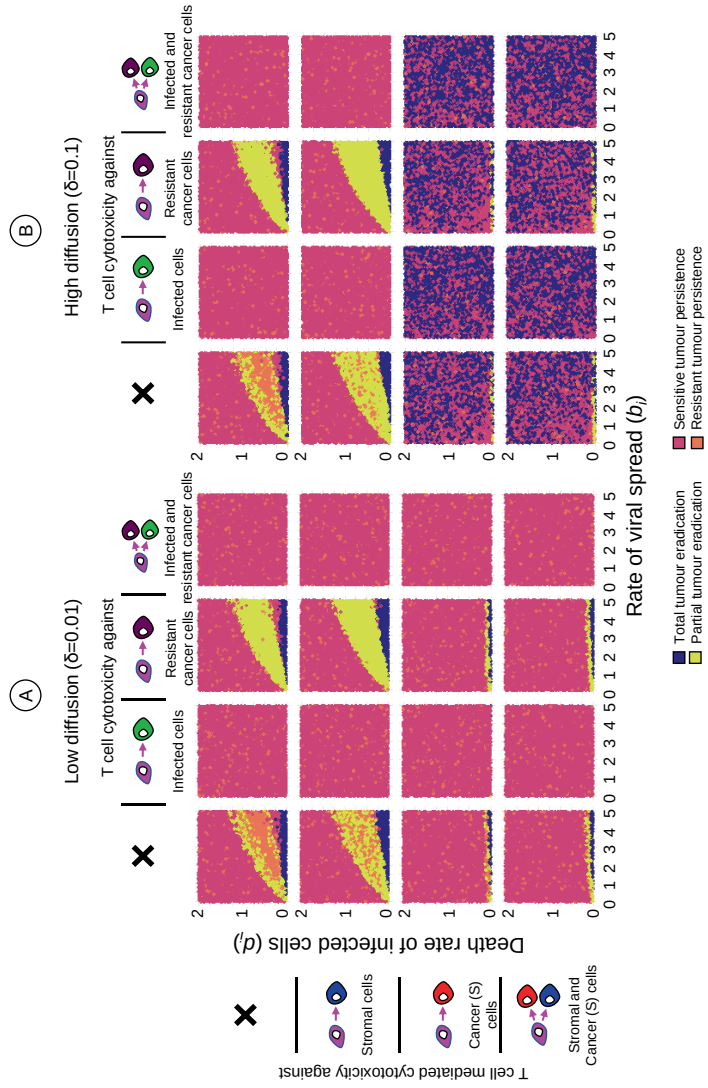

Supplementary Figure 2: Effect of T cell cytotoxicity against different cell types present in the tumour. For two diffusion rates of inflammatory molecules, the panels show how the outcome of oncolytic virotherapy is affected if the T cells target more than one cell type in the model. Each of the panel shows a possible scenario where the T cell cytotoxicity is targeted or not towards a specific cell type. The columns are arranged to show scenario with no cytotoxicity (first column), T cell cytotoxicity towards infected cells (second column), towards infection-resistant cells (third column), and towards both infected and infection-resistant cells (fourth column). The rows are arranged to show scenario with no cytotoxicity (first row), T cell cytotoxicity towards stromal cells (second row), towards infection-sensitive cancer cells (third row), and towards both stromal cells and infection-sensitive cells (fourth row). The combination of scenarios where T cell cytotoxicity acts towards one or more cell types results in sixteen scenarios ranging from no cytotoxicity (top left) to non-specific

cytotoxicity (bottom right). The sixteen scenarios were studied for (A) low ($\delta = 0.01$) and (B) high ($\delta = 0.1$) diffusion rates of inflammatory molecules. For each graph in the figure, 10,000 simulations were run for parameter combinations (bi, di) chosen randomly within the specified range. Each simulation is represented by a point, the colour of which indicates the therapeutic outcome. All model parameters were kept at their default values except the ones under investigation.

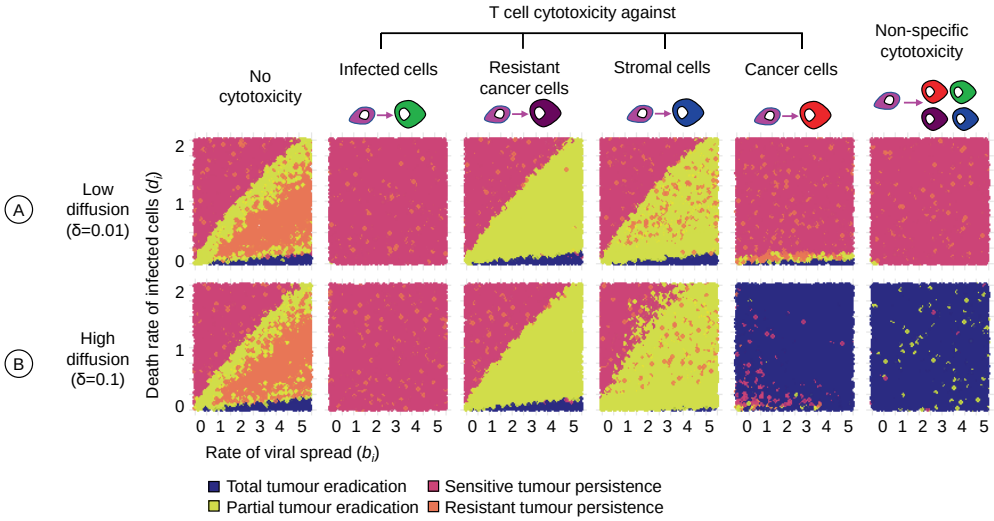

Supplementary Figure 3: Effect of T cell cytotoxicity against different cell types present in a 3D tumour model. The panels show how the outcome of oncolytic virotherapy is affected if the T cells do not target infection-sensitive cancer cells (the standard scenario) but other cells in a 3D version of the model. Six scenarios were studied for (A) low ($\delta = 0.01$) and (B) high ($\delta = 0.1$) diffusion rates of inflammatory molecules. The six scenarios considered (left to right) were: no cytotoxicity (absence of an immune response), and T cell cytotoxicity targeted towards either infected cells, infection-resistant cancer cells, stromal cells, infection-sensitive cancer cells, or all cell types present. For each graph in the figure, 10,000 simulations were run for parameter combinations (bi, di) chosen randomly within the specified range. Each simulation is represented by a point, the colour of which indicates the therapeutic outcome. All model parameters were kept at their default values except the ones under investigation.